



HAL
open science

Control of a Bioreactor with Quantized Measurements

Francis Mairet, Jean-Luc Gouzé

► **To cite this version:**

Francis Mairet, Jean-Luc Gouzé. Control of a Bioreactor with Quantized Measurements. Fages, François and Piazza, Carla. Formal Methods in Macro-Biology, 8738, Springer International Publishing, pp.47-62, 2014, Lecture Notes in Computer Science, 978-3-319-10398-3. 10.1007/978-3-319-10398-3_5 . hal-01092328

HAL Id: hal-01092328

<https://inria.hal.science/hal-01092328>

Submitted on 15 Dec 2014

HAL is a multi-disciplinary open access archive for the deposit and dissemination of scientific research documents, whether they are published or not. The documents may come from teaching and research institutions in France or abroad, or from public or private research centers.

L'archive ouverte pluridisciplinaire **HAL**, est destinée au dépôt et à la diffusion de documents scientifiques de niveau recherche, publiés ou non, émanant des établissements d'enseignement et de recherche français ou étrangers, des laboratoires publics ou privés.

Control of a bioreactor with quantized measurements

Francis Mairet and Jean-Luc Gouzé

INRIA BIOCORE, 2004 route des Lucioles,
BP 93, 06902 Sophia-Antipolis Cedex FRANCE
francis.mairet@inria.fr, jean-luc.gouze@inria.fr

Abstract. We consider the problem of global stabilization of an unstable bioreactor model (e.g. for anaerobic digestion), when the measurements are discrete and in finite number (“quantized”), with control of the dilution rate. The model is a differential system with two variables, and the output is the biomass growth. The measurements define regions in the state space, and they can be perfect or uncertain (i.e. without or with overlaps). We show that a quantized control may lead to global stabilization: trajectories have to follow some transitions between the regions, until the final region where they converge toward the reference equilibrium. On the boundary between regions, the solutions are defined as a Filippov differential inclusion.

Keywords: bioreactor, Haldane model, hybrid systems, differential inclusions, quantized output, control

1 Introduction

Classical control methods are often based on the complete knowledge of some outputs $y(t)$ of the system [21]. By complete, we mean that any output y_i is a real number, possibly measured with some noise δ_i . The control is then built with this (noisy) measurement. These tools have been successfully applied in many domains of science and engineering, e.g. in the domains of biosystems and bioreactors [10]. However, in these domains, detailed quantitative measurements are often difficult or impossible or too expensive. A striking example is the measurements of gene expression by DNA-chips, giving only a Boolean measure equal to on (gene expressed) or off (not expressed). In the domain of bioprocesses, it frequently happens that only a limited number or level of measurements are available (e.g. high, very high ...) because the devices only give a discretized semi-quantitative or qualitative measurement [6]. The measure may also be quantized by some physical device (as the time given by an analogical clock), and give as a result some number among a finite collection.

For this case of quantized outputs, the problem of control has also to be considered in a non-classical way: the control cannot be a function of the full continuous state variables anymore, and most likely will change only when the

quantized measurement changes. Moreover, the control itself could be quantized, due to physical device limitations.

The above framework has been considered by numerous works, having their own specificity: quantized output and control with adjustable “zoom” and different time protocols, [19], hybrid systems abstracting continuous ones (cf. [17] for many examples of theories and applications).

In this paper, we consider a classical problem in the field of bioprocesses: the stabilization of an unstable bioreactor model, this model being a simplified representation of anaerobic fermentation, towards its working set point. Anaerobic fermentation is one of the most employed process for (liquid) waste treatment [10]. The process (substrate and biomass are state variables) has two stable equilibria (and an unstable one, with a separatrix between the two basins of attractions of the respective stable equilibria), one being the (undesirable) washout of the culture ([15]). The goal is to globally stabilize the process toward the other locally stable reference equilibrium. The (classical) output is the biomass growth (through gaseous production), the control is the dilution rate (see [22] for a review of control strategies). For scalar continuous output, there exists many approaches based on well-accepted models ([7]), using constant or adaptive yield [18, 3]. Some original approaches make use of a supplementary competitor biomass [20].

In this paper, we suppose that the outputs are discrete or quantized: there are available in the form of finite discrete measurements. The precise models are described later: roughly, the simplest one is “perfect”, without noise, meaning that the true measure is supposed to be one of the discrete measurements, and that the transitions between two contiguous discrete measures are perfectly known. The next model is an uncertain model where the discrete measurements may overlap, and the true value is at the intersection between two quantized outputs. Remark that the model of uncertainty is different from the interval observers approaches ([2, 13]) for the estimation or regulation [1], where some outputs or kinetics are not well known, but upper or lower bounds are known. Moreover, in the interval observer case, the variables are classical continuous variables.

For this problem, the general approaches described above do not apply, and we have to turn to more tailored methods, often coming from the theory of hybrid systems, or quantized feedbacks (see above) ... We here develop our adapted “hybrid” approach. It has also some relations with the fuzzy modeling and control approach: see e.g. in a similar bioreactor process the paper [11]. We provide here a more analytic approach, and prove our results of stability with techniques coming from differential inclusions and hybrid systems theory [12]. Our work has some relations with theoretical qualitative control techniques used for piecewise linear systems in the field of genetic regulatory networks ([9]). The approach is also similar to the domain approaches used in hybrid systems theory, where there are some (controlled) transitions between regions, forming a transition graph [5, 14].

The paper is organized as follows: the first section describes the bioreactor model and the measurements models, and gives useful elements for the following.

In the second section, we explain what happens at the boundary between two discrete measurements, and define the control on this boundary, with the help of the Filippov definition of differential inclusion. We follow by giving the full solution of the problem in some cases and examples, with or without uncertainty.

2 Framework

2.1 Model presentation

In a perfectly mixed continuous reactor, the growth of biomass x limited by a substrate s can be described by the following system (see [4, 10]):

$$\begin{cases} \dot{s} = u(t)(s_{in} - s) - k\mu(s)x \\ \dot{x} = (\mu(s) - u(t))x \end{cases} \quad (1)$$

where s_{in} is the input substrate concentration, $u(t)$ the dilution rate, k the pseudo yield coefficient, and $\mu(s)$ the specific growth rate.

Given $\xi = (s, x)$, let us rewrite System (1) as $\dot{\xi} = f(\xi, u(t))$, where the dilution rate $u(t)$ is the manipulated input.

The specific growth rate $\mu(s)$ is assumed to be a Haldane function (i.e. with substrate inhibition) [7]:

$$\mu(s) = \bar{\mu} \frac{s}{k_s + s + s^2/k_i} \quad (2)$$

Parameters $\bar{\mu}, k_s, k_i$ describe the model and are positive. This function admits a maximum for a substrate concentration $s = \sqrt{k_s k_i} := \bar{s}$, and we will assume $\bar{s} < s_{in}$.

Lemma 1 *The solutions of System (1) with initial conditions in the positive orthant are positive and bounded.*

Proof. It is easy to check that the solutions stay positive. Now consider $z = s + kx$ whose derivative writes

$$\dot{z} = u(t)(s_{in} - z).$$

It follows that z is upper bounded by $\max(z(0), s_{in})$, and so is kx . Finally, if $s(t) > s_{in}$, then $\dot{s}(t) < 0$, therefore s is upper bounded by $\max(s(0), s_{in})$.

In the following, we will assume initial conditions within the interior of the positive orthant.

2.2 Quantized measurements

We consider that a growth proxy $y(\xi) = \alpha\mu(s)x$ of biomass growth is monitored (e.g. through gas production), but in a quantized way, in the form of a more or less qualitative measure: it can be levels (high, medium, low...) or discrete

measures. Finally, we only know that $y(\xi)$ is in a given range, or equivalently that ξ is in a given region (parameter α is a positive yield coefficient):

$$Y_i = \{\xi \in \mathbb{R}_+^2 : \underline{y}_i \leq y(\xi) \leq \bar{y}_i\}, \quad i = 1, \dots, n-1,$$

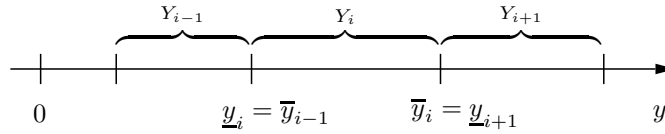
$$Y_n = \{\xi \in \mathbb{R}_+^2 : \underline{y}_n \leq y(\xi)\}.$$

where $0 = \underline{y}_1 < \underline{y}_2 < \dots < \underline{y}_n$ and $\bar{y}_1 < \bar{y}_2 < \dots < \bar{y}_{n-1}$. We will consider two cases:

- (A1). *Perfect* quantized measurements:

$$\bar{y}_i = \underline{y}_{i+1}, \quad \forall i = \{1, \dots, n-1\}.$$

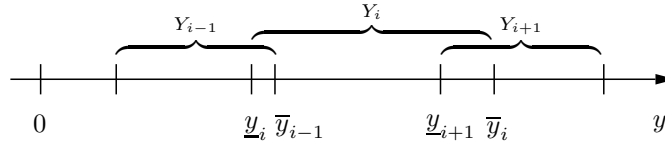
This corresponds to the case where there is no overlap between regions. The boundaries are perfectly defined and measured.



- (A2). *Uncertain* quantized measurements:

$$\underline{y}_i < \bar{y}_{i-1} < \underline{y}_{i+1}, \quad \forall i = \{2, \dots, n-1\}.$$

In this case, we have overlaps between the regions. In these overlaps, the measure is not deterministic, and may belong to two values.



For both cases, we define (open) regular domains:

$$\tilde{Y}_i := Y_i \setminus (Y_{i-1} \cup Y_{i+1}),$$

and (closed) switching domains:

$$Y_{i|i+1} := Y_i \cap Y_{i+1}.$$

For perfect measurements (A1), we have $\tilde{Y}_i = \text{int}Y_i$, and the switching domains $Y_{i|i+1}$ correspond to the lines $y(\xi) = \bar{y}_i = \underline{y}_{i+1}$. For uncertain measurements (A2), the switching domains $Y_{i|i+1}$ become the regions $\{\xi \in \mathbb{R}_+^2 : \underline{y}_{i+1} \leq y(\xi) \leq \bar{y}_i\}$.

In a switching domain $\xi \in Y_{i|i+1}$, we consider that the measurement is undetermined, i.e. either $\xi \in Y_i$ or $\xi \in Y_{i+1}$.

2.3 Quantized control

Given the risk of washout, our objective is to design a feedback controller that globally stabilizes System (1) towards a set-point. Given that measurements are quantized, the controller should be defined with respect to each region:

$$\xi(t) \in Y_i \Leftrightarrow u(t) = D_i, \quad i = 1, \dots, n. \quad (3)$$

Here D_i is the positive dilution rate in region i . This control scheme leads to discontinuities in the vector fields. Moreover, in the switching domains, the control is undetermined. Thus, solutions of System (1) under Control law (3) are defined in the sense of Filippov, as the solutions of the differential inclusion [12]:

$$\dot{\xi} \in H(\xi)$$

where $H(\xi)$ is defined on regular domains \tilde{Y}_i as the ordinary function $H(\xi) = f(\xi, D_i)$, and on switching domains $Y_{i|i+1}$ as the closed convex hull of the two vector fields in the two domains i and $i+1$:

$$H(\xi) = \overline{\text{co}}\{f(\xi, D_i), f(\xi, D_{i+1})\}.$$

Following [8, 9], a solution of System (1) under Control law (3) on $[0, T]$ is an absolutely continuous (w.r.t. t) function $\xi(t, \xi_0)$ such that $\xi(t, \xi_0) = \xi_0$ and $\dot{\xi} \in H(\xi)$ for almost all $t \in [0, T]$.

3 Model analysis with a constant dilution

For this case, the system is a classical ordinary differential equation in the whole space. When a constant dilution rate D is applied (i.e. $u(t) = D, \forall t \geq 0$), System (1) can present bistability, with a risk of washout. Let us denote $s_a(D)$ and $s_b(D)$ the two solutions, for $D \in (0, \mu(\bar{s}))$, of the equation $\mu(s) = D$, with $0 < s_a(D) < \bar{s} < s_b(D)$. For the Haldane growth rate defined by (2), we have:

$$s_a(D) = \frac{k_i}{2} \left(\frac{\bar{\mu}}{D} - 1 \right) - \sqrt{\left(\frac{k_i}{2} \left(\frac{\bar{\mu}}{D} - 1 \right) \right)^2 - k_s k_i}$$

$$s_b(D) = \frac{k_i}{2} \left(\frac{\bar{\mu}}{D} - 1 \right) + \sqrt{\left(\frac{k_i}{2} \left(\frac{\bar{\mu}}{D} - 1 \right) \right)^2 - k_s k_i}.$$

The asymptotic behavior of the system can be summarized as follows:

Proposition 1 *Consider System (1) with a constant dilution rate $u(t) = D$ and initial conditions in the interior of the positive orthant.*

(i) *If $D < \mu(s_{in})$, the system admits a globally exponentially stable equilibrium $\xi_a(D) = \left(s_a(D), \frac{s_{in} - s_a(D)}{k} \right)$.*

(ii) *If $\mu(s_{in}) < D < \mu(\bar{s})$, the system admits two locally exponentially stable*

equilibria, a working point $\xi_a(D) = \left(s_a(D), \frac{s_{in} - s_a(D)}{k} \right)$ and the washout $\xi_0 = (s_{in}, 0)$, and a saddle point $\xi_b(D) = \left(s_b(D), \frac{s_{in} - s_b(D)}{k} \right)$, see Figure 1.
 (iii) If $D > \mu(\bar{s})$, the washout $\xi_0 = (s_{in}, 0)$ is globally exponentially stable.

Proof. See [15].

For $D \in (0, \mu(\bar{s}))$, let us define:

$$y_j(D) = \frac{\alpha D}{k} [s_{in} - s_j(D)], \quad j = a, b.$$

$y_a(D)$ and $y_b(D)$ are the growth proxy obtained respectively at the equilibria $\xi_a(D)$ and $\xi_b(D)$ (if it exists)¹.

In order to design our control law, we need to provide some further properties of the system dynamics. In particular, we need to characterize $\dot{y}(\xi)$, the time derivative of $y(\xi)$ along a trajectory of System (1) with a constant dilution rate $u(t) = D$:

$$\dot{y}(\xi) = \alpha [D(s_{in} - s) - k\mu(s)x] \mu'(s)x + \alpha\mu(s)(\mu(s) - D)x.$$

Let us define the following functions:

$$g_D : s \mapsto \frac{\mu(s) - D}{k\mu'(s)} + \frac{D(s_{in} - s)}{k\mu(s)}$$

$$h_D^j : s \mapsto \frac{D(s_{in} - s_j(D))}{k\mu(s)}, \quad j = a, b.$$

In the (s, x) plane, $g_D(s)$, $h_D^a(s)$ and $h_D^b(s)$ represent respectively the nullcline $\dot{y}(\xi) = 0$ and the isolines $y(\xi) = y_a(D)$ and $y(\xi) = y_b(D)$ (i.e. passing through the equilibria $\xi_a(D)$ and $\xi_b(D)$), see Figure 1. Knowing that the nullcline $\dot{y}(\xi) = 0$ is tangent to the isoline $y(\xi) = y_a(D)$ (resp. $y(\xi) = y_b(D)$) at the equilibrium point $\xi_a(D)$ (resp. $\xi_b(D)$), we will determine in the next lemma the relative positions of these curves, see Fig. 1.

Lemma 2 (i) For $s \in (0, \bar{s})$, we have $g_D(s) \geq h_D^a(s)$: the nullcline $\dot{y}(\xi) = 0$ is over the isoline $y(\xi) = y_a(D)$
 (ii) For $s \in (\bar{s}, s_{in})$, we have $g_D(s) \leq h_D^b(s)$: the nullcline $\dot{y}(\xi) = 0$ is below the isoline $y(\xi) = y_b(D)$.

Proof. See Appendix.

This allows us to determine the monotonicity of $y(\xi)$ in a region of interest (for the design of the control law).

Lemma 3 Consider System (1) with a constant dilution rate $u(t) = D$. For $\xi \in \mathbb{R}_+^2$ such that $y_b(D) < y(\xi) < y_a(D)$, we have $\dot{y}(\xi) > 0$.

Proof. See Appendix.

¹ if $D < \mu(s_{in})$, $\xi_b(D)$ does not exist and $y_b(D) < 0$.

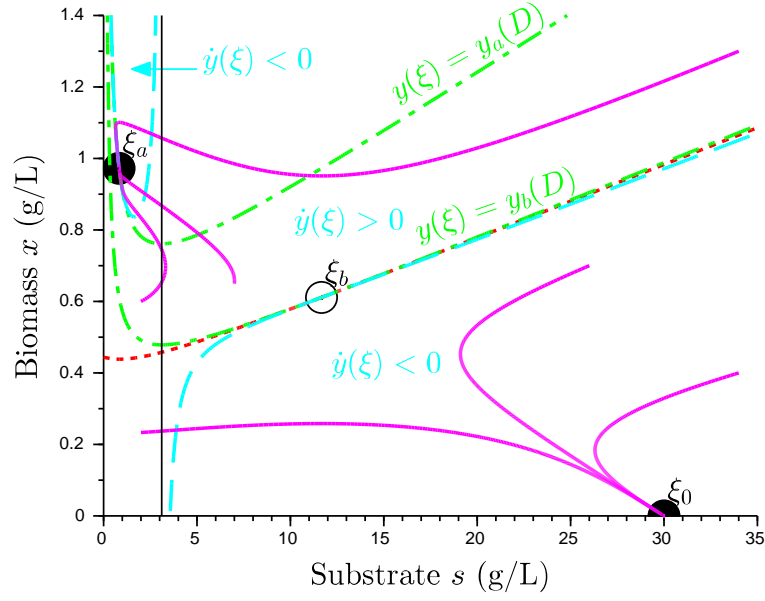


Fig. 1. Phase portrait of System (1) with a constant dilution rate $u(t) = D \in (\mu(s_{in}); \mu(\bar{s}))$. Magenta lines: trajectories, cyan dashed lines: nullcline $\dot{y}(\xi) = 0$, green dash dotted lines: isolines $y(\xi) = y_a(D)$ and $y(\xi) = y_b(D)$, red dotted line: separatrix, black vertical line: $s = \bar{s}$, dark circles: stable equilibria, open circle: unstable equilibrium.

4 Control with quantized measurements

4.1 Control design

Our goal is to globally stabilize the system towards the stable equilibrium corresponding to D_n . Number n is the number of measurements (see section 2.2) and the control is such that $D_1 < D_2 < \dots < D_n$. The last dilution rate D_n is chosen because of its high productivity, it verifies the case (ii) of Prop. 1. We consider the following control law, based on the quantized measurements $y(\xi)$:

$$\forall t \geq 0, \quad \xi(t) \in Y_i \Leftrightarrow u(\xi) = D_i, \quad (4)$$

given that the following conditions are fulfilled:

$$y_b(D_i) < \underline{y}_i \quad i = 1, \dots, n, \quad (5)$$

$$y_a(D_i) > \bar{y}_i \quad i = 1, \dots, n-1, \quad (6)$$

$$y_a(D_n) > \bar{y}_{n-1}. \quad (7)$$

These conditions make the equilibrium $\xi_a(D_n)$ globally stable, as we will see below. In Section 5.1, we will precise how to choose the D_i such that these conditions hold.

In order to prove the asymptotic behavior of System (1) under Control law (4-7), the study will be divided into three steps:

- the dynamics in one region,
- the transition between two regions,
- the global dynamics.

This approach is similar to those deducing the global dynamics from a “transition graph” of possible transitions between regions.

4.2 Dynamics in one region with a given dilution: exit of domain

We first focus on a region Y_i , $i < n$. A constant dilution D_i - such that Conditions (5-6) for i hold - is applied. These conditions guarantee that the stable operating equilibrium for this dilution (see Proposition 1) is located in an upper region Y_j , $j > i$, while the saddle point is located in a lower region Y_k , $k < i$. This allows us to establish the following lemma:

Lemma 4 *For any $i \in \{1, \dots, n-1\}$, consider System (1) under a constant control $u(t) = D_i$, such that Conditions (5-6) for i hold. All solutions with initial conditions in Y_i leaves this domain, crossing the boundary $y(\xi) = \bar{y}_i$.*

Proof. Let us consider the function $V(\xi) = y_a(D_n) - y(\xi)$ on Y_i . Given Conditions (5-6), we get $\forall \xi \in Y_i$:

$$y_b(D_i) < \underline{y}_i < y(\xi) < \bar{y}_i < y_a(D_i).$$

Since a constant dilution rate D_i is applied, we can apply Lemma 3 to conclude that $\dot{y}(\xi) > 0$.

Thus, $V(\xi)$ is decreasing on Y_i . Recalling that the trajectories are also bounded (Lemma 1), we can apply LaSalle invariance theorem [16] on the domain $\Omega_1 := \{\xi \in Y_i \mid x \leq \max(z(0), s_{in})/k, s \leq \max(s(0), s_{in})\}$. Given that the set of all the points in Ω_1 where $\dot{V}(\xi) = 0$ is empty, any trajectory starting in Ω_1 will leave this region. The boundaries $x = \max(z(0), s_{in})/k$ and $s = \max(s(0), s_{in})$ are repulsive (see Proof of Lemma 1). Finally, the boundary $y(\xi) = \underline{y}_i$ corresponds to the maximum of $V(\xi)$ on Ω_1 , so every trajectory will leave this domain, crossing the boundary $y(\xi) = \bar{y}_i$.

4.3 Transition between two regions

Now we will characterize the transition between regions (as we have seen above, the intersection can be either a simple curve in the case of perfect measurements, or a region with non empty interior in the uncertain case):

Lemma 5 *For any $i \in \{1, \dots, n-1\}$, consider System (1) under Control law (4) with Conditions (5-6) for $i, i+1$ ². All trajectories with initial conditions in $Y_i \cup Y_{i+1}$ enter the regular domain \tilde{Y}_{i+1} .*

Proof. First, we consider $i \neq n-1$. We will follow the same reasoning as for the previous lemma, applying Lasalle theorem on a domain

$$\Omega_2 := \{\xi \in \text{int}\mathbb{R}_+^2 \mid x \leq \max(z(0), s_{in})/k, s \leq \max(s(0), s_{in}), \bar{y}_{i-1} < y(\xi) < y^\dagger\}$$

with $\bar{y}_i < y^\dagger < \underline{y}_{i+2}$. We can show that the functional $V(\xi) = y_a(D_n) - y(\xi)$ is decreasing on Y_i whenever $u = D_i$. Similarly, $V(\xi)$ is also decreasing on Y_{i+1} whenever $u = D_{i+1}$. Now under Control law (4), we have shown that $V(\xi)$ is decreasing on the regular domains \tilde{Y}_i and \tilde{Y}_{i+1} . $V(\xi)$ is a regular C^1 function, and can be differentiated along the differential inclusion. On the switching domains Y_{i+1} , we have:

$$\dot{V}(\xi) \in \overline{\text{co}} \left\{ \frac{\partial V}{\partial x} f(\xi, D_i), \frac{\partial V}{\partial x} f(\xi, D_{i+1}) \right\} < 0.$$

Thus, $V(\xi)$ is decreasing on Ω_2 . Following the proof of Lemma 4 concerning the boundaries, we can deduce that every trajectory will reach the boundary $y(\xi) = y^\dagger$, i.e. it will enter \tilde{Y}_{i+1} .

For $i = n-1$, taking $\bar{y}_{n-1} < y^\dagger < y_a(D_n)$, we can show similarly that $V(\xi)$ is decreasing on Ω_2 so every trajectory will enter the region \tilde{Y}_n .

Following the same proof, we can show that the reverse path is not possible, in particular for the last region:

² or if $i = n-1$, Conditions (5) for $n-1, n$, Condition (6) for $n-1$, and Condition (7).

Lemma 6 Consider System (1) under Control law (4) with Conditions (5) for $n - 1, n$, Condition (6) for $n - 1$, and Condition (7). The regular domain \tilde{Y}_n is positively invariant.

4.4 Global dynamics

Proposition 2 Control law (4-7) globally stabilizes System (1) towards the point $\xi_a(D_n)$.

Proof. From Lemmas 5 and 6, we can deduce that every trajectory will enter the regular domain \tilde{Y}_n , and that this domain is positively invariant.

System (1) under a constant control $u(t) = D_n$ has two non-trivial equilibria (see Proposition 1): $\xi_a(D_n)$, and $\xi_b(D_n)$. The growth proxy at these two points satisfy $y_a(D_n) > \bar{y}_{n-1}$ and $y_b(D_n) < \underline{y}_n$ (Conditions (5,7)), so there is only one equilibrium in \tilde{Y}_n : $\xi_a(D_n)$. Moreover, it is easy to check that \tilde{Y}_n is in the basin of attraction of $\xi_a(D_n)$, therefore all trajectories will converge toward this equilibrium.

5 Implementation of the control law

5.1 How to fulfill Conditions (5-7)

The global stability of the control law is based on Conditions (5-7). We consider the case where the regions are imposed (by technical constraints of the measurements) and we want to find the different dilution rates D_i such that these conditions hold. The approach may be analytic or graphical, and will be described elsewhere.

For example, for perfect measurements (A1) with equidistribution, it can be shown that it will always be possible to implement the desired control law, i.e. it is always possible to find a set of dilution rates D_i such that Conditions (5-7) hold, whenever the measurement resolution is good enough (i.e. the number of regions is high enough). The result is illustrated by the simulations below.

5.2 Simulations

As an example, we consider the anaerobic digestion process, where the methane production rate is measured. Parameters, given in Table 1, are inspired from [7] (considering only the methanogenesis step). Our objective is to stabilize the equilibrium $\xi_a(D^*)$, with $D^* = 0.47 \text{ d}^{-1}$ (which corresponds to a productivity of 92% of the maximal productivity).

For uncertain measurements, we use discrete time simulation. At each time step t_k (with $\Delta t = 0.05 \text{ d}$), when $\xi(t_k)$ is in a switching region $Y_{i|i+1}$, we choose randomly the control $u(t_k)$ between D_i and D_{i+1} . In this case, we perform various simulations for a same initial condition.

Trajectories for various initial conditions are represented in the phase portrait for perfect and uncertain measurements, see Figure 2 and Figure 3.

Table 1. Parameter values used for simulation.

Parameter	Value
$\bar{\mu}$	0.74 d ⁻¹
k_s	0.59 g.L ⁻¹
k_i	16.4 g.L ⁻¹
k	30
α	11 L CH ₄ .g ⁻¹
s_{in}	30 g.L ⁻¹

On top of both figures, the number of regions (three regions only) is too small in order to stabilize the given set-point $\xi_a(D^*)$: it is not possible to choose dilution rates such that Conditions (5-7) hold. In this case, some trajectories do not converge towards the set-point. Some regions have transitions towards the upper region, but also towards the lower one. There are sliding modes. This aspect will be further discussed in the next subsection.

On bottom of both figures, with one more region (four measurements), we can define a set of dilution rates such that Conditions (5-7) are fulfilled. The transition graph is deterministic (there is only one transition from a region to the upper one).

Actually, given the following perfect measurement set (considering equidistant region):

$$\bar{y}_i = \underline{y}_{i+1} = \frac{i}{n-1} \bar{y}_n, \quad i = 1, \dots, n-1, \quad \text{with} \quad \bar{y}_n = 4 \text{ L CH}_4 \cdot \text{L}^{-1} \cdot \text{d}^{-1},$$

we can choose the following dilution rates:

$$D_1 = 0.19 \text{ d}^{-1}, \quad D_2 = 0.29 \text{ d}^{-1}, \quad D_3 = 0.4 \text{ d}^{-1}, \quad D_4 = 0.47 \text{ d}^{-1}.$$

For uncertain measurements, we increased each upper bound and decreased each lower bound by 10%. It appears that the same dilution rates can be chosen.

Thus, all the trajectories converge towards the set-point (see Figure 3).

5.3 When Conditions are not verified: risk of failure

We here detail what happens if Conditions (5-7) are not fulfilled, and in particular if there is a risk of washout. This point is illustrated by the top figures of Fig. 2 and Fig. 3.

First, given the previous analysis of the system, one can easily see that only the condition $y_b(D_1) < \underline{y}_1$, i.e. $D_1 < \mu(s_{in})$ is necessary to prevent a washout, so D_1 can be chosen with a safety margin in order to avoid such situation. Now, if Condition (6) does not hold for some i , the stable equilibrium $\xi_a(D_i)$ will be located in the region Y_i , so some trajectories can converge towards this point instead of going to the next region. On the other hand, if Condition (5) is not

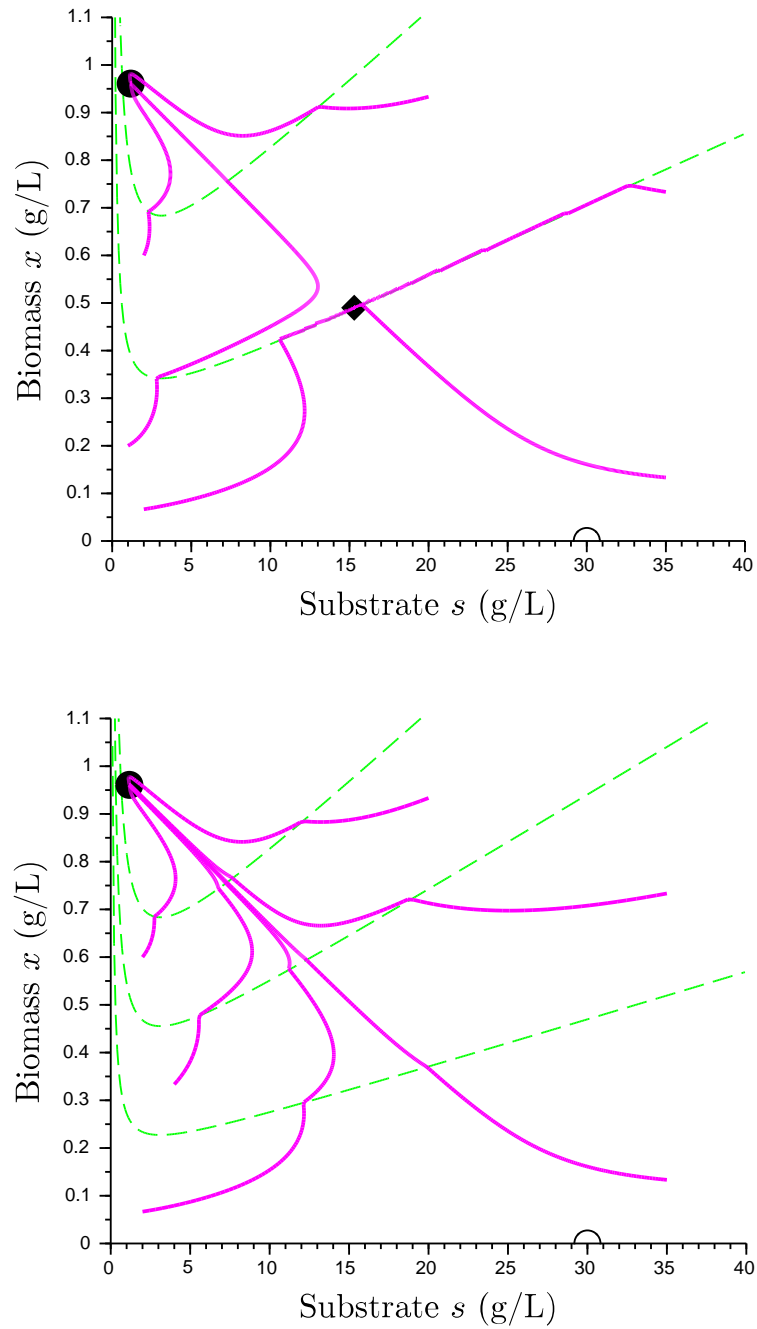


Fig. 2. Trajectories (magenta lines) with Control law (4) for various initial conditions in the phase portrait, in the case of perfect measurements. Top: Conditions (5-7) are not fulfilled, some trajectories converge towards a singular equilibrium point (black diamond) with a sliding mode. Bottom: Conditions (5-7) are fulfilled, all the trajectories converge towards the set-point (dark circle). Open circle: washout. The frontiers are represented by the green dashed lines.

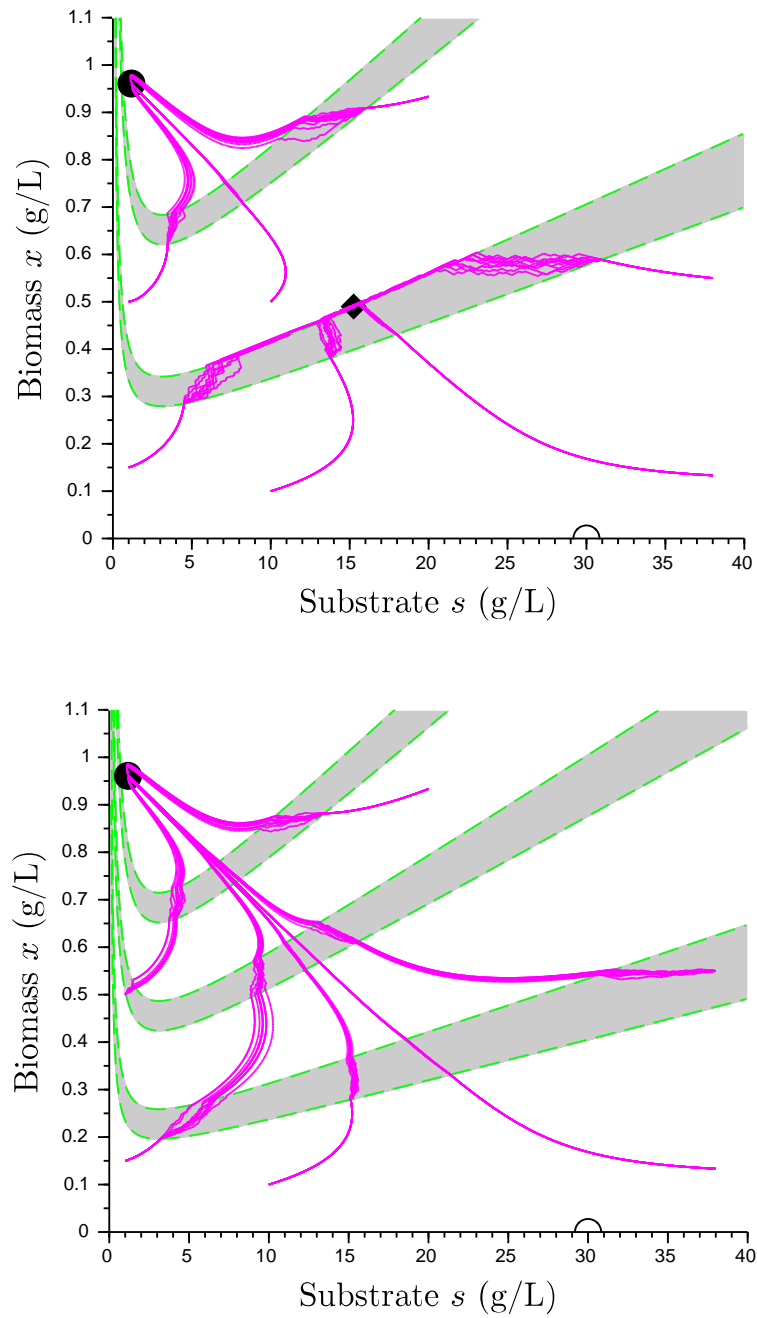


Fig. 3. Trajectories (magenta lines) with Control law (4) for various initial conditions in the phase portrait, in the case of uncertain measurements. Top: Conditions (5-7) are not fulfilled, some trajectories converge towards a singular equilibrium point (black diamond) with a sliding mode. Bottom: Conditions (5-7) are fulfilled, all the trajectories converge towards the set-point (dark circle). The frontiers are represented by the green dashed lines, switching regions are colored in gray. In these gray regions, the system is not deterministic. Open circle: washout.

fulfilled for some $i > 1$, the unstable equilibrium $\xi_b(D_i)$ will be located in the region Y_i , and thus a trajectory can stay in a switching domain. Given that z converges towards s_{in} , such trajectory will converge towards the intersection between the switching domain and the invariant manifold $z = s_{in}$ (see Figure 2, Figure 3 on top):

- For perfect measurements (A1), this gives rise to a sliding mode and the convergence towards a singular equilibrium point.
- For uncertain measurements (A2), all the trajectories converge towards a line segment. In our simulation, they actually also converge towards a singular equilibrium point.

In all the cases, the trajectories converge towards a point or a line segment. Although it is not desired, this behavior is particularly safe (given that there is theoretically no risk of washout). Moreover, undesired equilibrium can easily be detected and the dilution rates can be changed accordingly (manually or through a supervision algorithm).

6 Conclusion

Given the quantized measurements, we were able to design (under some conditions) a control based on regions and transition between regions. These tools are similar to the ones of piecewise linear systems, and it is possible to draw a transition graph showing all the possible transitions. Moreover, we have seen that for some cases, singular behaviors (sliding modes) are possible on the boundaries between regions. We think that this kind of control on domains, and design of the resulting transition graph, is a promising approach, that we want to deepen in future works. This approach could be generalized to others classical systems, e.g. in mathematical ecology.

References

1. Alcaraz-Gonzalez, V., Harmand, J., Rapaport, A., Steyer, J., Gonzalez-Alvarez, V., Pelayo-Ortiz, C.: Robust interval-based regulation for anaerobic digestion processes. *Water Science & Technology* 52(1-2), 449–456 (2005)
2. Alcaraz-González, V., Harmand, J., Rapaport, A., Steyer, J., Gonzalez-Alvarez, V., Pelayo-Ortiz, C.: Software sensors for highly uncertain wwtps: a new approach based on interval observers. *Water Research* 36(10), 2515–2524 (2002)
3. Antonelli, R., Harmand, J., Steyer, J.P., Astolfi, A.: Set-point regulation of an anaerobic digestion process with bounded output feedback. *Control Systems Technology, IEEE Transactions on* 11(4), 495–504 (2003)
4. Bastin, G., Dochain, D.: *On-line estimation and adaptive control of bioreactors*. Elsevier (1990)
5. Belta, C., Habets, L.: Controlling a class of nonlinear systems on rectangles. *Automatic Control, IEEE Transactions on* 51(11), 1749–1759 (2006)

6. Bernard, O., Gouzé, J.L.: Non-linear qualitative signal processing for biological systems: application to the algal growth in bioreactors. *Mathematical Biosciences* 157(1), 357–372 (1999)
7. Bernard, O., Hadj-Sadok, Z., Dochain, D., Genovesi, A., Steyer, J.P.: Dynamical model development and parameter identification for an anaerobic wastewater treatment process. *Biotechnology and bioengineering* 75(4), 424–438 (2001)
8. Casey, R., de Jong, H., Gouzé, J.L.: Piecewise-linear models of genetic regulatory networks: Equilibria and their stability. *Journal of Mathematical Biology* 52, 27–56 (2006)
9. Chaves, M., Gouzé, J.L.: Exact control of genetic networks in a qualitative framework: the bistable switch example. *Automatica* 47(6), 1105–1112 (2011)
10. Dochain, D.: *Automatic control of bioprocesses*, vol. 28. John Wiley & Sons (2010)
11. Estaben, M., Polit, M., Steyer, J.P.: Fuzzy control for an anaerobic digester. *Control Engineering Practice* 5(9), 1303–1310 (1997)
12. Filippov, A.F.: *Differential Equations with Discontinuous Righthand Sides*. Kluwer Academic Publishers, Dordrecht (1988)
13. Gouzé, J.L., Rapaport, A., Hadj-Sadok, M.Z.: Interval observers for uncertain biological systems. *Ecological modelling* 133(1), 45–56 (2000)
14. Habets, L., van Schuppen, J.H.: A control problem for affine dynamical systems on a full-dimensional polytope. *Automatica* 40(1), 21–35 (2004)
15. Hess, J., Bernard, O.: Design and study of a risk management criterion for an unstable anaerobic wastewater treatment process. *Journal of Process Control* 18(1), 71–79 (2008)
16. LaSalle, J.P.: *The Stability of Dynamical Systems*. CBMS-NSF Regional Conference Series in Applied Mathematics, Society for Industrial and Applied Mathematics (1976)
17. Lunze, J., Lamnabhi-Lagarigue, F.: *Handbook of hybrid systems control: theory, tools, applications*. Cambridge University Press (2009)
18. Mailleret, L., Bernard, O., Steyer, J.P.: Nonlinear adaptive control for bioreactors with unknown kinetics. *Automatica* 40(8), 1379–1385 (2004)
19. Nesic, D., Liberzon, D.: A unified framework for design and analysis of networked and quantized control systems. *Automatic Control, IEEE Transactions on* 54(4), 732–747 (2009)
20. Rapaport, A., Harmand, J.: Biological control of the chemostat with nonmonotonic response and different removal rates. *Mathematical Biosciences and Engineering* 5(3), 539–547 (2008)
21. Sontag, E.D.: *Mathematical control theory: deterministic finite dimensional systems*, vol. 6. Springer (1998)
22. Steyer, J., Bernard, O., Batstone, D.J., Angelidaki, I.: Lessons learnt from 15 years of ica in anaerobic digesters. *Instrumentation, Control and Automation for Water and Wastewater Treatment and Transport Systems IX* 53(4), 25–33 (2006)

7 Appendix

Proof of Lemma 2

Let us define $\varphi_D^j(s) := g_D(s) - h_D^j(s)$ for $j = a, b$. We have:

$$\begin{aligned}\varphi_D^j(s) &= \frac{D(s_j(D) - s)}{k\mu(s)} + \frac{\mu(s) - D}{k\mu'(s)}, \\ \varphi_D^{j'}(s) &= \frac{1}{k}(\mu(s) - D) \left(\frac{1}{\mu(s)} - \frac{\mu''(s)}{\mu'(s)^2} \right) - D(s_j(D) - s) \frac{\mu'(s)}{k\mu(s)^2}.\end{aligned}$$

First, we consider $\varphi_D^a(s)$ on $(0, \bar{s})$. Given that $\mu(s)$ is increasing and concave on this interval, we get $\varphi_D^{a'}(s) < 0$ on $(0, s_a(D))$, and $\varphi_D^{a'}(s) > 0$ on $(s_a(D), \bar{s})$. Moreover, we have $\varphi_D^a(s_a(D)) = 0$, so $\varphi_D^a(s) \geq 0$ on $(0, \bar{s})$, which proves (i).

Now we want to determine the sign of $\varphi_D^b(s)$ on $(\bar{s}, +\infty)$. For this purpose, we consider the equation $\varphi_D^b(s) = 0$. By replacing $\mu(s)$ and its derivative by their analytic expressions, this equation becomes:

$$\frac{s_a(D)}{k_i} s^2 - 2k_s s + k_s s_b(D) = 0.$$

Given that $s_a(D)s_b(D) = k_s k_i$, the equation $\varphi_D^b(s) = 0$ has only one root $s = s_b(D)$. Moreover, we have:

$$\lim_{s \searrow \bar{s}} \varphi_D^b(s) = -\infty \quad \text{and} \quad \lim_{s \rightarrow +\infty} \varphi_D^b(s) = -\infty.$$

Given that $\varphi_D^b(s)$ is continuous on $(\bar{s}, +\infty)$, we finally conclude that on this interval, $\varphi_D^b(s) \leq 0$, i.e. $g_D(s) \leq h_D^b(s)$. \square

Proof of Lemma 3

First, given that $g_D(s)$ represent the nullcline $\dot{y}(\xi) = 0$, we can check that we have (see Figure 1):

$$\dot{y}(\xi) > 0 \text{ on } \{\xi \in \text{int}\mathbb{R}_+^2 \mid s < \bar{s}, x < g_D(s)\} \cup \{\xi \in \text{int}\mathbb{R}_+^2 \mid s > \bar{s}, x > g_D(s)\}.$$

Recalling that $h_D^a(s)$ and $h_D^b(s)$ are respectively the isolines $y(\xi) = y_a(D)$ and $y(\xi) = y_b(D)$, Lemma 2 allows to conclude that for $\xi \in \mathbb{R}_+^2$ such that $y_b(D) < y(\xi) < y_a(D)$, we have $\dot{y}(\xi) > 0$. \square